

Permeability of Oxygen and Carbon Dioxide Through Pinholes in Barrier Coatings

Petri Johansson*

Tampere University

Johanna Lahti

Tampere University

Jorma Vihinen

Tampere University

Jurkka Kuusipalo

Tampere University

ABSTRACT

Packaging materials are typically made of multilayer structures combining polymers, metals and inorganic materials. Multilayer structures are selected in order to optimize the thickness and performance in packaging applications. Atomic layer deposited (ALD) aluminium oxide (Al_2O_3) layer provides good barrier properties against oxygen and carbon dioxide gases i.e. permeation of gases through ALD coated polymer films will reduce remarkably. The target was to study the effect of pinholes on the oxygen and carbon dioxide permeability of ALD coated extrusion-coated packaging paper. Pinholes were artificially generated by ultra violet (UV) laser drilling through the polymer layer prior to Al_2O_3 ALD coating. The results show, that even one pinhole through the structure can destroy the excellent barrier properties of the film material. It was found out that the size of a pinhole affects detrimentally the oxygen gas permeation through the material. According to the results, there is a linear correlation between permeation rate of oxygen gas and area of pinhole, thus, oxygen barrier level can be calculated and adjusted by the size of pinhole.

KEY WORDS

atomic layer deposition, aluminium oxide, pinhole, permeability, gas barrier, packaging

***Petri Johansson**

Corresponding Author

petri.johansson@tuni.fi

INTRODUCTION

There is a need to create more ecological structures with excellent barrier properties to packages, because the environmentally friendly aspects are growing worldwide [1]. Atomic layer deposited (ALD) aluminium oxide (Al_2O_3) layer is a potential barrier coating layer in packaging materials. Barrier properties of Al_2O_3 ALD layer have been studied recently and the possibility to low permeations have been proved [2]. In the current solutions gas and liquid barrier properties of packages are mainly formed with aluminium foil or barrier polymer layers. A typical thickness of aluminium foil in liquid packages is nowadays 6 μm , but the layer can be thicker (9-12 μm or even higher) when the amount of pinholes is critical [3, 4, 5].

Al_2O_3 ALD can also replace metallised plastic films, which are commonly used barrier coating material for polymer packages. Typically, metallised (Al_2O_3 or SiOx) film is biaxially-oriented polyethylene terephthalate (BOPET). The thickness of metallised coating of Al_2O_3 or SiOx barrier layer is typically 0,05 μm , which is about the same thickness as Al_2O_3 ALD layer. [4]

The focus of this work was to study the effect of pinholes on barrier performance of different kinds of polymer and Al_2O_3 ALD structures before and after the pinhole generation. The flow of gas through the package material is much slower, if there is no easier and faster

route (pinholes) to the gas. Even one pinhole may destroy the excellent barrier properties of the structure. [6]

Because the target is to study the effect of artificially made pinhole/pinholes on permeability of the structure, the structure has to be originally absolutely pinhole free [7]. In order to make sure that there are no pinholes in the structure, the polymer layer has to be thick enough [8]. Al-metallized polymer film typically has pinholes in aluminium layer [9]. Ideally, an Al_2O_3 ALD layer does not contain any pinholes, if the polymer substrate underneath is pinhole-free. It has been proved that the barrier values might be very low, if there is an Al_2O_3 layer on top of polymer substrate [10, 11].

MATERIALS AND METHODS

The study was started by producing different kinds of papers, polymers and ALD-structures with pinholes. Extrusion coating polymer [low density polyethylene (LDPE) / polyethylene terephthalate (PET) / polylactic acid (PLA)] was varied. A pigment coated paper (Lumiflex 80 g/m^2 , Stora Enso) was used as substrate. The machine calendered non-pigment coated side of the paper was extrusion coated in pilot line (Figure 1) at Tampere University of Technology (TUT) using a glossy chill roll, which gave smooth surface texture. The

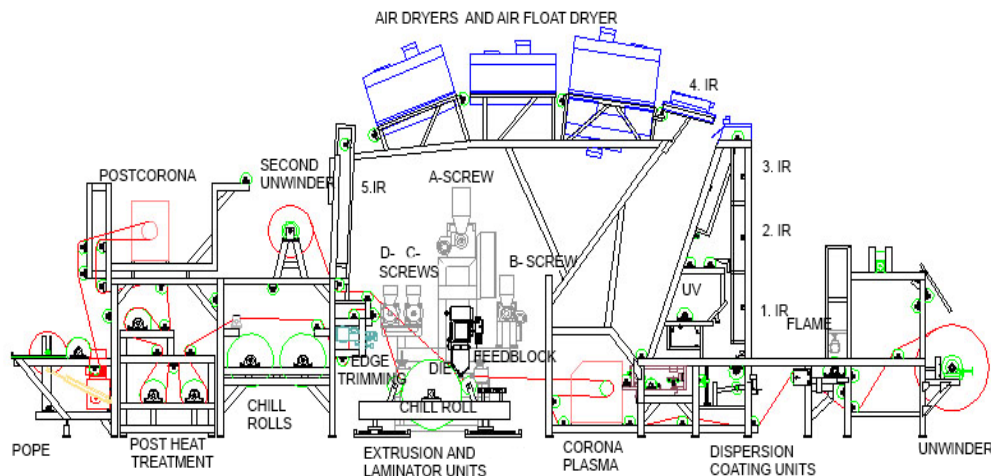


Fig. 1: (Co)Extrusion coating and lamination pilot line at TUT.

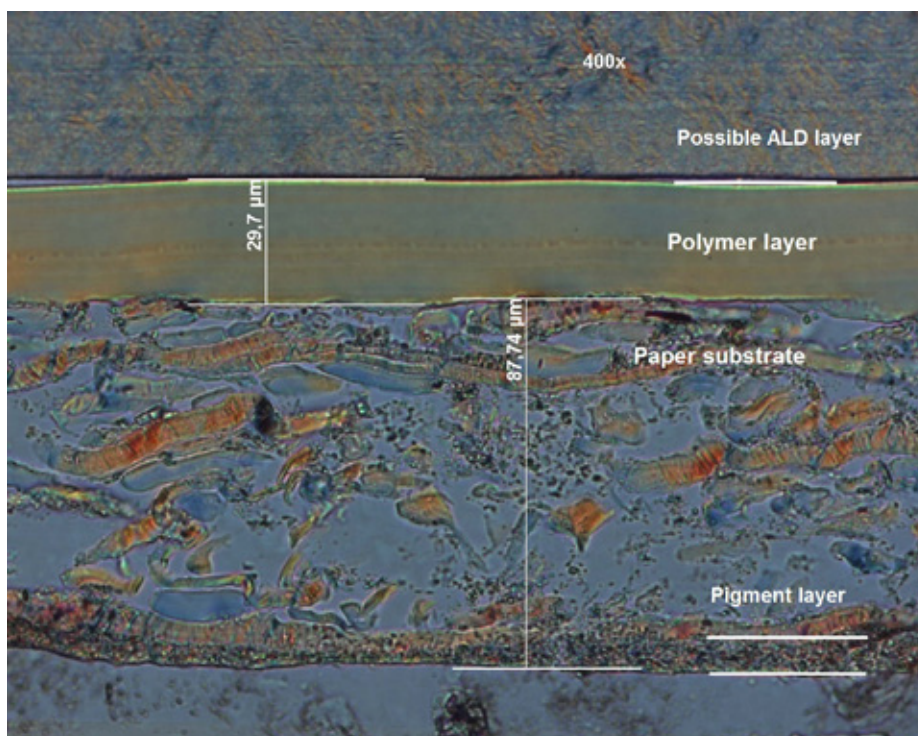


Fig. 2: Cross-sectional structure of extrusion coated paper sample with the thickness of paper and polymer layer (ALD layer is not visible).

Al_2O_3 layer was deposited by ALD on the extrusion coated paper in order to create the following structure: paper // LDPE or PET or PLA // Al_2O_3 .

The adhesion between polymer and paper substrate was perfect with all the studied polymers. The thickness of extrusion coated polymer layer was adjusted so (LDPE 35 g/m², PET 39 g/m² and PLA 38 g/m²) that the undrilled film was absolutely pinhole free. In Figure 2 is shown a cross cut of a typical extrusion coated paper sample in this study. The fibre side of paper is extrusion coated and the ALD layer would be on top of the polymer layer.

Extrusion coated paper/polymer -samples were cut into sheets with size of 13 cm x 13 cm followed by UV laser drilling of pinholes. In the first set of drilled pinholes (A), the diameter size was targeted to be as small as possible. The diameter size in the second set of drilled pinholes (B) was a little larger than in the first set. All three polymer coatings had pinholes of two sizes (A and B) and three different amounts of pinholes (0, 1 and 2).

Ultraviolet (UV) laser can be used to drill pinholes with controlled shapes and sizes through polymer and paper, e.g. extrusion coated paper. This opens a possibility to generate pinholes of accurate size and further on to evaluate the effect of them on gas permeation through polymer/paper packaging structures. In food packages, relevant gases to study are oxygen (O_2) and carbon dioxide (CO_2). [12]

The UV laser drilling made at TUT. The laser was Eolite Boreas with a wavelength of 343 nm and frequency of 10 kHz. The scanner was Scanlab HuryScan II 14 with Ftheta 103 mm. The power (\varnothing 10 μm and \varnothing 20 μm) was 206 mW (23.3 A). The power efficiency measured by Coherent Fieldmax II and the type of sensor was PM30. The pinholes of \varnothing 10 μm were made by percussion drilling (five seconds, around 50 000 pulses). The pinholes of \varnothing 20 μm were made by helical drilling (100 times with speed of 10 mm/s).

After the pinholes had been made, the samples were Al_2O_3 ALD coated on top of the polymer surface. Batch Al_2O_3 ALD coating process (Beneq TFS 500)

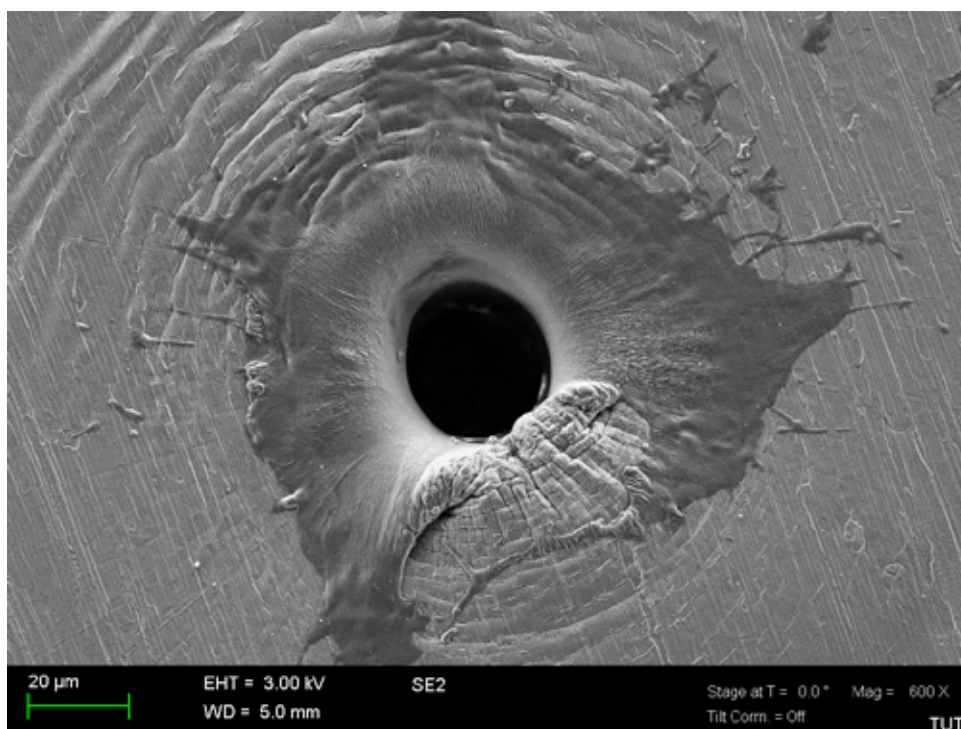


Fig 3: An Al₂O₃ ALD coated surface with splashed polymer on top.

was made at Lappeenranta University of Technology (LUT). The thickness of Al₂O₃ layer was targeted to be 40 – 50 nm (450 cycles at temperature of 75°C) Precursor gases were trimethylaluminum (TMA) with purity of 98% (Volatec) and ozone (O₃ was produced with an ozone generator at LUT) [13].

Scanning electron microscopy (SEM) was used to determine the real size and shape of drilled pinholes. SEM pictures of the samples were taken after the permeability measurements. The used SEM device at TUT was ZEISS ULTRAplus (Ultra high resolution field emission scanning electron microscope). The samples were glued by carbon on the aluminum stubs and the surfaces of samples were sputtered with gold coating to avoid the sample charging in the SEM studies.

During the experiments it was observed that drilling the pinholes through paper/polymer/Al₂O₃ – structure turned out to be unsuccessful procedure, because the laser melted and splashed the molten polymer on top of an Al₂O₃ layer (Figure 3). Thus, the pinholes were generated before the ALD coating.

After the Al₂O₃ ALD coating process, the samples were sent from LUT to TUT in no-touch boxes to the barrier measurements. Permeability through the structures was measured with gases of O₂ and CO₂. Both measurements were made in conditions of 23°C and 0% relative humidity (RH) with two parallel samples. The area of measuring in the sample was 5 cm².

The measurements of oxygen transmission rate (OTR) were made by Mocon Ox-Tran 2/21 SS according to the standard ASTM D3985. The oxygen content of the used gas was 10% (nitrogen as a carrier gas). The measurements of carbon dioxide transmission rate (CO₂TR) were made by Mocon Permatran-C 4/41 according to the standard ASTM F2476 – 05.

The amount of different structures in samples outlined to 18 set points. In Table 1 is the list of the produced samples in this study.

Permeation of oxygen and carbon dioxide through the ALD coated multilayer structure can be divided into a three-stage process including [14]:

Table 1: The sample structures with targeted size of pinholes.

PE ref	pigment coated paper - LDPE, no pinholes.
PE ald	pigment coated paper - LDPE - Al ₂ O ₃ ALD, no pinholes.
PE 1 A	pigment coated paper - LDPE - Al ₂ O ₃ ALD, 1 pinhole Ø size of 10 µm.
PE 1 B	pigment coated paper - LDPE - Al ₂ O ₃ ALD, 1 pinhole Ø size of 20 µm.
PE 1 A	pigment coated paper - LDPE - Al ₂ O ₃ ALD, 2 pinholes Ø size of 10 µm.
PE 2 B	pigment coated paper - LDPE - Al ₂ O ₃ ALD, 2 pinholes Ø size of 20 µm.
PET ref	pigment coated paper - PET, no pinholes.
PET ald	pigment coated paper - PET - Al ₂ O ₃ ALD, no pinholes.
PET 1 A	pigment coated paper - PET - Al ₂ O ₃ ALD, 1 pinhole Ø size of 10 µm.
PET 1 B	pigment coated paper - PET - Al ₂ O ₃ ALD, 1 pinhole Ø size of 20 µm.
PET 2 A	pigment coated paper - PET - Al ₂ O ₃ ALD, 2 pinholes Ø size of 10 µm.
PET 2 B	pigment coated paper - PET - Al ₂ O ₃ ALD, 2 pinholes Ø size of 20 µm.
PLA ref	pigment coated paper - PLA, no pinholes.
PLA ald	pigment coated paper - PLA - Al ₂ O ₃ ALD, no pinholes.
PLA 1 A	pigment coated paper - PLA - Al ₂ O ₃ ALD, 1 pinhole Ø size of 10 µm.
PLA 1 B	pigment coated paper - PLA - Al ₂ O ₃ ALD, 1 pinhole Ø size of 20 µm.
PLA 2 A	pigment coated paper - PLA - Al ₂ O ₃ ALD, 2 pinholes Ø size of 10 µm.
PLA 2 B	pigment coated paper - PLA - Al ₂ O ₃ ALD, 2 pinholes Ø size of 20 µm.

1. sorption of the penetrant onto the flat material
2. diffusion of the penetrant through material matrix along the concentration gradient
3. desorption of the penetrant from the opposite side of the material

The molecular diffusion of gases across a polymer membrane is defined by Fick's first law of diffusion as shown in Equation 1 [15].

Where,

P = permeability

ΔQ = amount of gas transmitted in the given time

T = thickness

Δt = time

A = area

P_1 / P_2 = pressure

The permeation of gases (Fick's first law) is described in Figure 4.

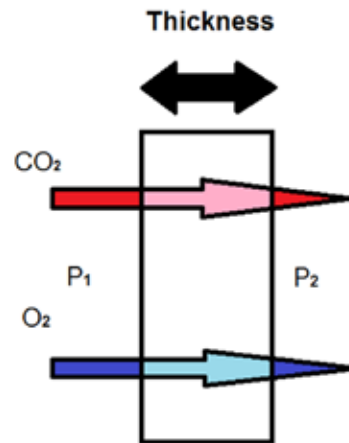


Figure 4. Gas diffusion (from 1) through a membrane (to 2).

The oxygen and carbon dioxide permeation through the polymer structure of food package (mainly to fruits and vegetables) have been studied [16, 17, 18]. In the studies the permeation through the package material (membrane and the artificially made pinholes) increased when the size of pinhole increased.

RESULTS AND DISCUSSION

The size of pinholes

The permeation of O² and CO² gases through the structures with pinholes was studied. The main target was to find out the difference between pinhole-free structure and structure with pinholes. Each laser drilled pinhole was detected and images were taken with optical microscope or SEM. The real size of a drilled pinhole was determined using the images, because it was difficult to distinguish how large the pinholes through the structure were. That is why all pinholes are demonstrated also with backlight. In the optical microscopic Figures 5 and 6 are shown the Ø 10 µm pinholes from the polymer/paper –samples.

The real area of a drilled hole through the structure looks to be near of the anticipated diameter of 10 µm. The light, which comes through the pinhole, gives a good vision of the pinhole size in polymer. The actual area of the drilled hole in polymer layer is important to know as precisely as possible when comparing the size of the pinhole and the permeation (oxygen or carbon dioxide) through the structure. The optical microscopic Figures 7 and 8 show the Ø 20 µm pinholes from the polymer/paper –samples.

The actual area of a drilled hole through the structure seems to be near of the targeted Ø 20 µm. The size of drilled hole in paper side is not so important when thinking of gas permeability because polymer layer mainly provides the gas barrier. In the optical microscopic Figures 9 and 10 are drilled pinholes in the polymer layers from the paper side.

The area of a drilled hole in a paper (from paper side) is greater than the planned Ø 10 µm or Ø 20 µm. That does not affect the barrier properties of the structure, because paper is a poor barrier layer against the oxygen and carbon dioxide.

The correlation between pinhole size and gas barrier

Because the permeation through the substrate (Figure 4) is depending (not only Al₂O₃ ALD layer) on the polymer material (LDPE / PET / PLA) and permeating gas (O² / CO²), the measured permeation values do not have correlation to each other when the material or gas is different [19].

Hypothetically, the gas barrier properties of these kind of structures are mainly provided by Al₂O₃ ALD layer [20]. In this study, the pigment coated paper substrate was always the same. The gas barrier properties of paper are negligible when comparing it to the polymer structures. The thickness of polymer layer was about 30-40 µm and the thickness of Al₂O₃ was about 45 nm. In the formula of Fick's first law, the thickness is in numerator. That means the measured values are mainly recording the barrier properties of an Al₂O₃ layer with and without pinholes.

In previous Figures (5, 6, 7, 8, 9 and 10) were presented the sizes of drilled holes in the polymer layer and they are very close to the targeted Ø 10 µm or Ø 20 µm diameters. Diameters were used to calculate the size of pinholes. In Table 2 are shown the measured permeation values of oxygen and carbon dioxide through the samples.

Because there was remarkable difference between the measured values in OTR of parallel samples 3A // 3B and 4A // 4B, the size of drilled pinholes had to be confirmed by SEM. The Figure 11 shows the size of pinhole in sample 3B (PE 1 A) and the Figure 12 shows the size of pinhole in sample 4A (PE 1 B). SEM images show the differences between sizes of pinholes.

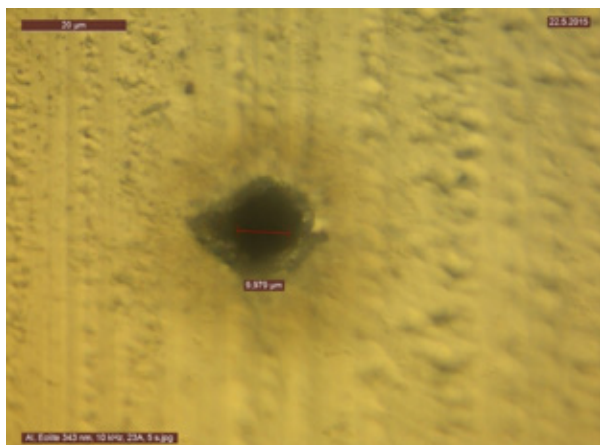


Figure 5: The sample with Ø 10 µm pinhole from polymer side.

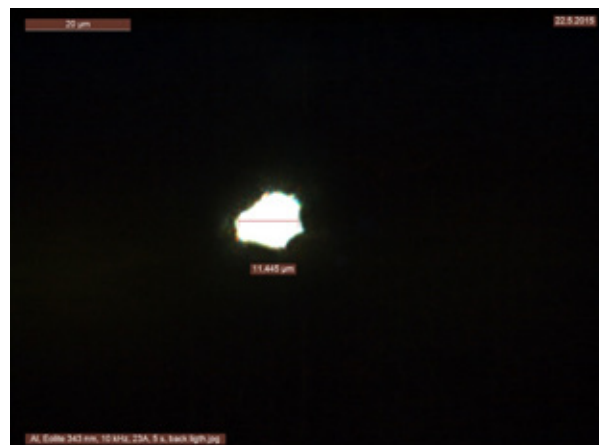


Figure 6: The sample with Ø 10 µm pinhole from polymer side with back light.

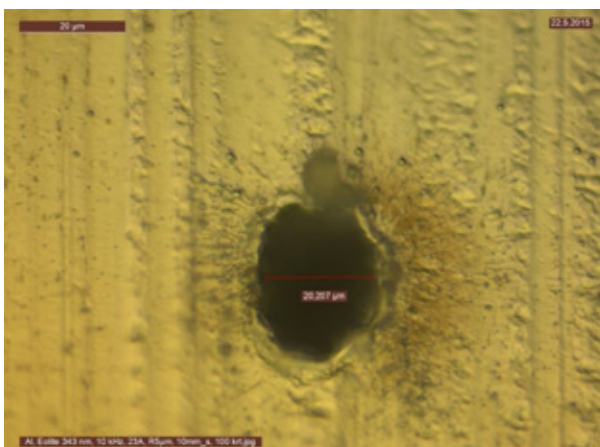


Figure 7: The sample with Ø 20 µm pinhole from polymer side.

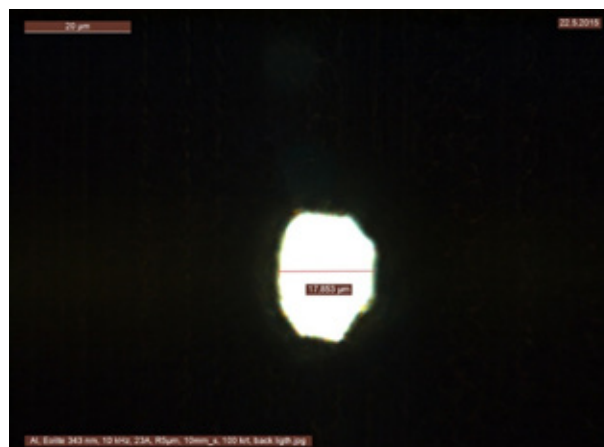


Figure 8: The sample with Ø 20 µm pinhole from polymer side with back light.



Figure 9: The sample with Ø 10 µm pinhole from paper side.

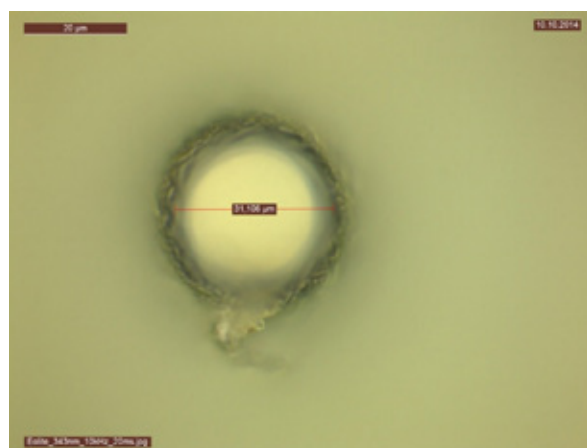


Figure 10: The sample with Ø 20 µm pinhole from paper side.

Table 2: The measured permeation values of oxygen and carbon dioxide through the samples.

Size = 5 cm ²	OTR 23°C, 0%RH		cm ³ /m ² /d	CO ₂ TR 23°C, 0%RH		cm ³ /m ² /d
	A	B	Average	A	B	Average
1=PE ref	791	744	768	12418	10192	11305
2=PE ald	141	413	277	2024	3304	2664
3=PE 1 A	347	2373	2373	3801	4918	4360
4=PE 1 B	16616	8304	12460	50000	50000	50000
5=PE 1 A	340	2189	2189	3653	5249	4451
6=PE 2 B	15779	20103	17941	50000	50000	50000
7=PET ref	80	76	78	1022	920	971
8=PET ald	24	12	18	161	97	129
9=PET 1 A	20037	5394	12716	50000	50000	50000
10=PET 1 B	20000	10777	15389	50000	50000	50000
11=PET 2 A	12786	20000	16393	50000	50000	50000
12=PET 2 B	20021	25152	22587	50000	50000	50000
13= PLA ref	263	287	280	2821	2628	2725
14=PLA ald	35	45	40	191	121	156
15=PLA 1 A	7737	4227	5982	19205	5611	12408
16=PLA 1 B	15078	10062	12570	50000	50000	50000
17=PLA 2 A	14174	13486	13830	20549	50000	35275
18=PLA 2 B	22158	20709	21434	50000	50000	50000

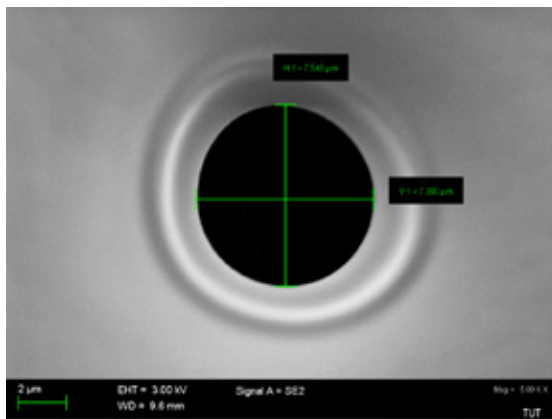


Figure 11. LDPE, the size of the hole in sample 3B.

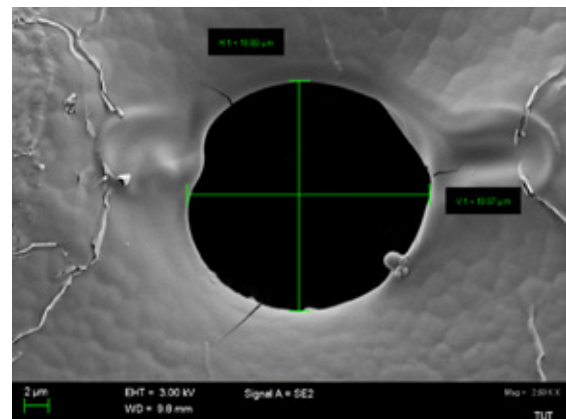


Figure 12. LDPE, the size of the hole in sample 4A

When it is possible to identify the hole and the permeability of a specific gas through the hole, it is possible to find out how much gas is flowing through the structure and through the pinhole.

The difference between the dimensions of the holes explains the remarkable difference in OTR between the samples. In Figure 11, the sample's OTR was 2373 cm³/m²/d and in Figure 12, the sample's OTR was 16616 cm³/m²/d. The larger the pinhole area through the whole structure is, the greater is the permeation of oxygen through the sample. The formula after pinhole areas were calculated as follows:

$$\frac{\pi \times [(height + width/2) \times (height + width/2)]}{4}$$

When calculating the areas of the pinholes, in Figure 11 (with the height of 7,548 µm and the width of 7,392 µm) it is 43,8 µm² and in Figure 12 (with the height of 18,99 µm and the width of 19,97 µm) it is 298 µm².

The OTR of the samples and the measured areas of the pinholes in the samples correlate rather well, when comparing the ratio of larger and smaller pinhole. The measured OTR [cm³/m²/d] values were 16616 and 2373 and measured pinhole areas [µm²] were 298 and 43,8; thus the corresponding ratios are as follows:

$$\text{OTR -ratio: } \frac{16616}{2373} = 7,0$$

$$\text{Pinhole area -ratio: } \frac{298}{43,8} = 6,8$$

In Figure 13 the OTR and pinhole area results are compared.

The curve in Figure 13 was achieved by using Excel linear trendline. According to Figure 13, the curve across the X-axis near origin (48,6), which shows that linear correlation between the area of pinholes and OTR is strong.

If there should be a pinhole in the SEM picture, but the measured OTR value is on the level, which is the same as the structure with no pinhole, the assumed pinholes have to be studied with SEM more carefully. Figure 14 (sample 5A, PE 1 A) and Figure 15 (sample 5A, PE 1 A) show the SEM images taken from the same spot. It is difficult to observe if there is a pinhole or just a crater in Figure 14. Instead, the Figure 15 shows clearly that it is a crater.

By using different kind of illumination (Figure 14 and Figure 15), it can be noted that there is no pinhole in sample 5A, which explains the similar OTR values to pinhole free samples (2A or 2B). Figure 16 and Figure 17 (reference to Figure 16) show photographs of exactly the same pinhole but using different kinds of illuminations. The actual pinhole through the polymer is smaller (Figure 17) than it looks on the surface image (Figure 16).

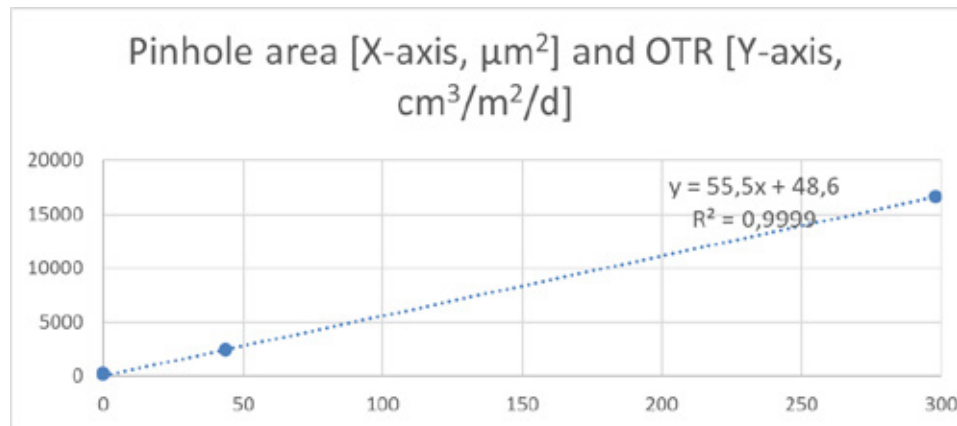


Figure 13. OTR and pinhole area of studied samples 2A (PE ald), 3B (PE 1 A) and 4A (PE 1 B).

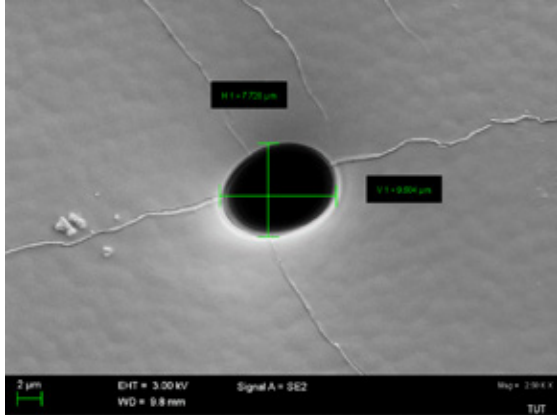


Figure 14. LDPE, the size of the assumed hole in sample 5A

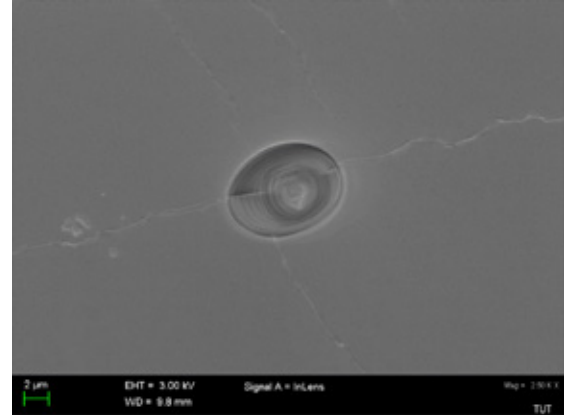


Figure 15. LDPE, there is a crater (not hole) in sample 5A

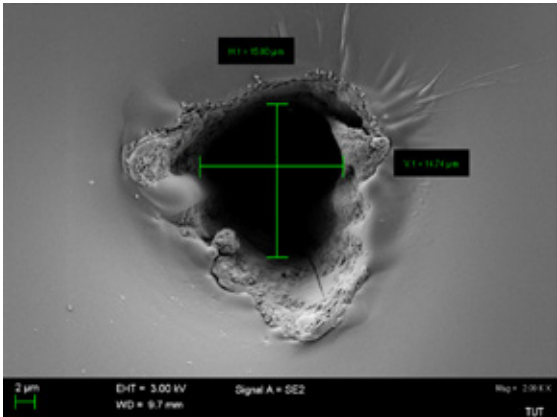


Figure 16. PET, the size of the hole in sample 11B

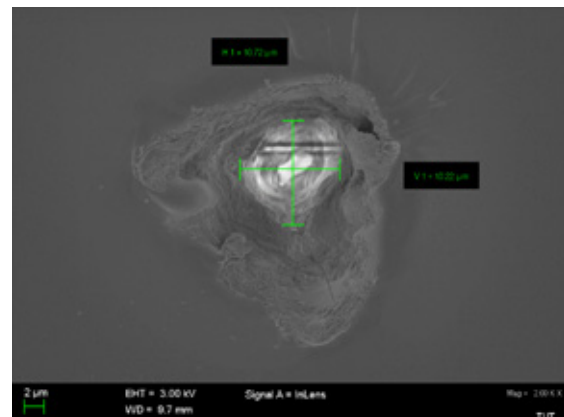


Figure 17. PET, the size of the crater (and hole) in sample 11B

Influence of pinhole to OTR and CO₂TR

In order to study the effect of pinholes on permeation with different polymers, OTR and CO₂TR measurements were made for all samples. Measurements were made both for pinhole-free and pinhole-containing samples. Figure 18 shows oxygen permeation through the measured structures. In Table 1 and Table 2 are the explanation of codes shown in Figure 18 and Figure 19.

As seen in Figure 18, Al₂O₃ layer reduces greatly the oxygen permeation values with all the studied polymer coatings. The effect is different depending on the polymer coating like the previous studies have shown [20]. It is obvious that if the substrate is pinhole-free, the oxygen permeation value is much smaller than with the exactly same kind of

sample with one or two pinholes. When comparing the LDPE samples with 1 small pinhole and 1 large pinhole, it can be noticed that the sample with larger pinhole has also higher permeation values. The ratio of the size of hole in LDPE layer and the OTR is also almost constant as shown in Figure 13. The increasing permeation when increasing the amount of holes can be observed when comparing PET and PLA samples with one or two pinholes.

Figure 19 shows the carbon dioxide permeation through the samples. The maximum detection limit of CO₂TR measuring device is 50000. In Figure 19 the samples, which have permeation value over this detection limit, are marked with value 50000. The samples have exactly the same kind of structures and handling like in the oxygen permeation test (Figure 18).

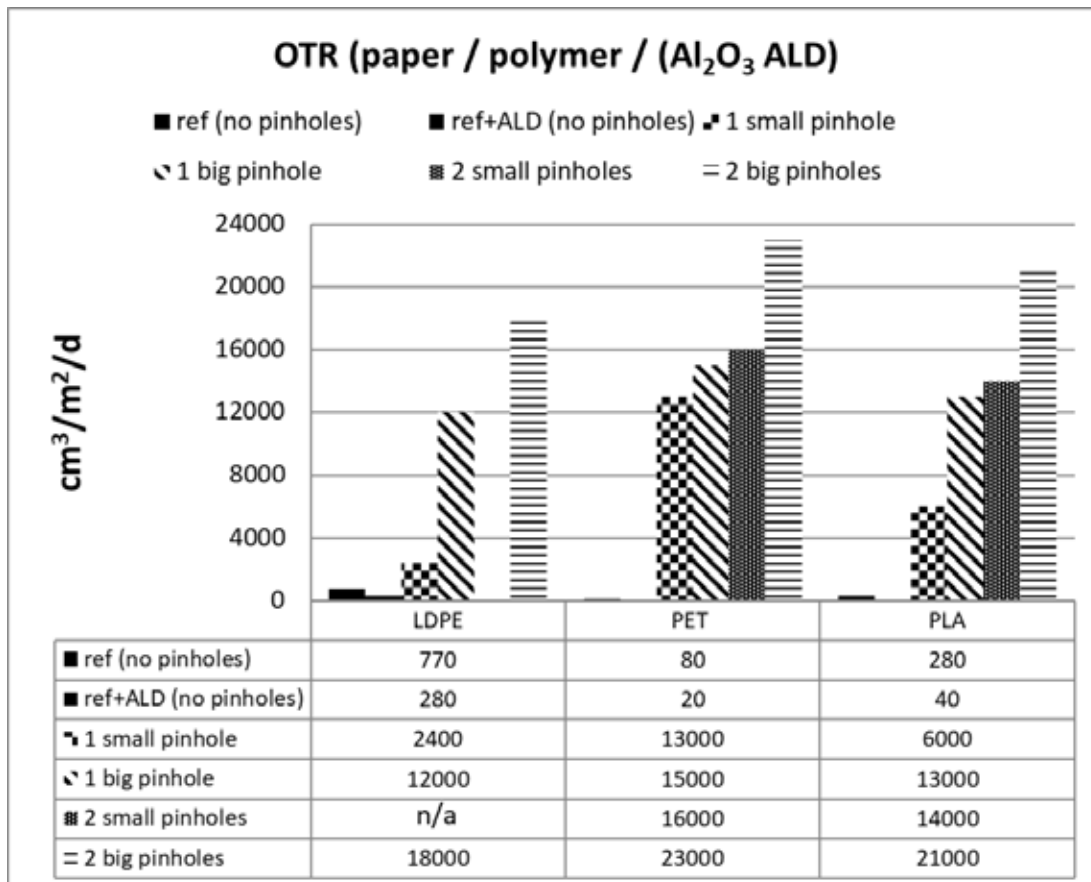


Figure 18. OTR of paper/polymer (/Al₂O₃ ALD) samples with and without pinholes.

Results in Figure 19 show that Al_2O_3 layer reduces the carbon dioxide permeation values with all polymer coatings. If the pinhole free substrates with and without Al_2O_3 layer are compared, it can be noticed that the lowest CO_2 permeation value can be achieved with PET. The results also show that the pinholes vastly increase the CO_2 permeation values with all the studied polymers. When comparing LDPE samples with 1 small and 1 large pinhole, it can be seen that the sample with larger pinhole has over 10 times greater carbon dioxide permeation values. Also with samples having 2 pinholes, the permeation values are very high. Similar effect can be observed with PLA when comparing samples with 1 small pinhole and 1 large or 2 pinholes. However, in PET samples both the smaller and larger pinholes gave permeation values over 50000. Thus, they can

not be compared to each other. These permeation measurements indicate that the size of the pinhole does not solely define the amount of gas permeation, because the permeation value with oxygen and carbon dioxide is different for LDPE, PET and PLA with the approximately same size of pinholes. The permeation of oxygen and carbon dioxide is different for LDPE, PET and PLA films, which have an effect of total permeation with pinholes.

The following comparisons and calculations between reference polymer and Al_2O_3 ALD/polymer coatings were made to more precisely explain differences between polymer materials and used gases.

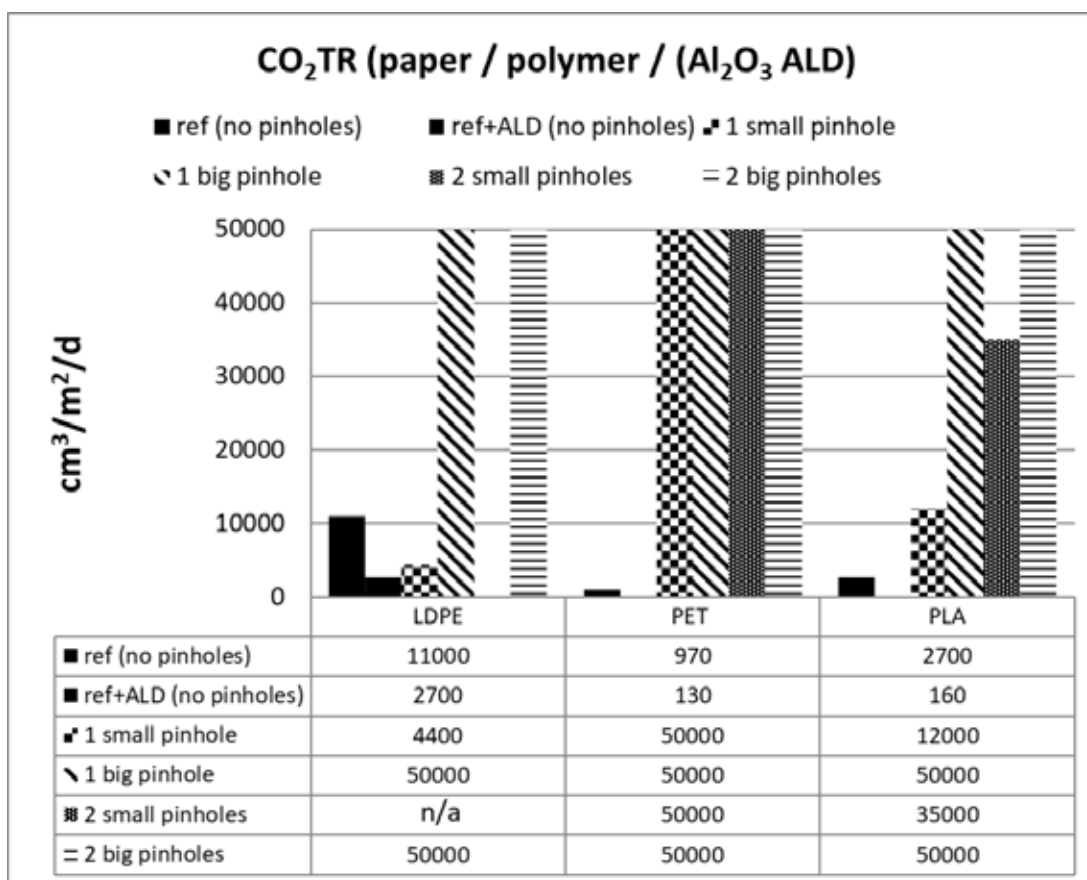


Figure 19. CO_2TR of paper/polymer (Al_2O_3 ALD) samples with and without pinholes.

Polymer	gas -ratio: $\frac{\text{without Al}_2\text{O}_3 \text{ ALD}}{\text{with Al}_2\text{O}_3 \text{ ALD}} =$	
LDPE	OTR -ratio: $\frac{768}{277} = 2,8$	CO ₂ TR -ratio: $\frac{11305}{2664} = 4,2$
PET	OTR -ratio: $\frac{78}{18} = 4,3$	CO ₂ TR -ratio: $\frac{921}{129} = 7,5$
PLA	OTR -ratio: $\frac{280}{40} = 7,0$	CO ₂ TR -ratio: $\frac{2725}{156} = 17,5$

According to polymer comparisons, PLA coating had the best improvement in gas barrier due to Al₂O₃ ALD coating and LDPE coating the weakest. As far as the gases are compared, the carbon dioxide permeation values decreased relatively more than the oxygen permeation values.

CONCLUSIONS

This study focused on extrusion coated paper which was Al₂O₃ ALD coated in order to enhance barrier properties of oxygen and carbon dioxide. It was noticed that both oxygen and carbon dioxide permeability was decreased with all the studied extrusion coating polymers (LDPE, PET and PLA). The effect is relatively different depending on the used polymer coating and the permeating gas. Al₂O₃ coating affects carbon dioxide permeability even more than oxygen permeability.

In this study, the effect of pinholes on the gas flow of oxygen and carbon dioxide through the Al₂O₃ ALD coated polymer film was evaluated. The results clearly show that even one pinhole can destroy the barrier properties of the structure. It was observed that the OTR value and the diameter of a pinhole had a linear correlation. Similar conclusion could not be made in the case of carbon dioxide permeation.

It can be concluded that by choosing the amount and diameter of pinholes, the permeation of different gases can be tailored. This could open new possibilities in packaging material development. With UV-laser it is possible to drill pinholes with specific size to polymer layer, but in practice the sizes of pinhole were not identical. In future, the challenge

is to make pinholes with exactly the same size. When studying the difference between polymers, it would be interesting to measure the permeation through pinholes with exactly the same size. Furthermore, it would be beneficial to study correlation between pinholes and WVTR to understand more selective barrier properties.

ACKNOWLEDGEMENTS

We wish to thank the Nanomend project (EU FP7 programme, Grant Agreement 280581) and Stora Enso for their financial and material support.

REFERENCES

- [1] Terhi Hirvikorpi. "Thin Al₂O₃ barrier coatings grown on bio-based packaging materials by atomic layer deposition" D.S. Thesis. VTT publications 770, Espoo. 2011. <http://urn.fi/URN:ISBN:978-951-38-7751-4>
- [2] M.S.J. Hashmi. "Comprehensive Materials Processing," in 13 Volume set. Elsevier. 2014.
- [3] FAQs – Tetra Pak Recycling. 2018. <http://www.tetrapakrecycling.co.uk/faqs.asp>. (Accessed: 8 October 2018)
- [4] Jurkka Kuusipalo et al. Paper and paperboard converting, second edition. Papermaking Science and Technology. 2008. ISBN 978-952-5216-28-8.
- [5] Lee Murray. "The impact of foil pinholes and flex cracks on the moisture and oxygen barrier of flexible packaging," in TAPPI PLACE Conference, Las Vegas, Nevada, 2005.
- [6] Kit L. Yam. Packaging technology, third edition. Wiley. 2009.

- [7] Timothy K. Minton, Bohan Wu, Jianming Zhang, Ned F. Lindholm, Jennifer O'Patchen, Steven M. George, Markus D. Groner. "Protecting polymers with atomic layer deposition coatings," in ACS Applied Materials and Interfaces. 2010.
- [8] Karyn L. Jarvis, Peter J. Evans. "Growth of thin barrier films on flexible polymer substrates by atomic layer deposition," in Thin Solid Films 624 (2017) 111-135.
- [9] Haeyong Jung, Choong Hyo Jang, In Seok Yeo, Tae-Ho Song. "Investigation of gas permeation through Al-metallized film for vacuum insulation panels," in International Journal of Heat and Mass Transfer 56 (2013) 436-446.
- [10] W. A. Barrow, E. R. Dickey. "Roll-to-Roll ALD deposition of Al₂O₃ barrier layers on PET," in Lotus Applied Technology, Hillsboro, OR.
- [11] Philipp Maydannik, Tommi Kääriäinen, Kimmo Lahtinen, David C. Cameron, Mikko Söderlund, Pekka Soininen, Petri Johansson, Jurkka Kuusipalo, Lorenza Moro, Ziaghui, Zeng. "Roll-to-roll atomic layer deposition process for flexible electronics encapsulation applications" in Journal of Vacuum Science & Technology A: Vacuum, Surfaces, and Films, Volume 32, Issue 5, 2014.
- [12] Nanomend. Project full title: "Nanoscale defect detection, cleaning and repair for large area substrates" Grant agreement number 280581. 2012 – 2015. <http://www.nanomend.eu>.
- [13] Philipp Maydannik. "Roll-to-Roll atomic layer deposition process for flexible electronics applications." D.S. thesis. Lappeenranta University of Technology, Mikkeli, 2015. <http://www.doria.fi/handle/10024/109216>.
- [14] Kimmo Lahtinen. "Statistical WVTR models for extrusion-coated webs in various atmospheric conditions." D.S. thesis. Tampere University of Technology, Tampere, 2010. <http://dspace.cc.tut.fi/dpub/bitstream/handle/123456789/6582/lahtinen.pdf>.
- [15] Wolf R. Vieth. Diffusion in and through polymers. Principles and Applications. USA. Univ. Press. 1991.
- [16] Svetlana Fishman, V. Rodov, S. Ben-Yehoshua. "Mathematical model for perforation effect on oxygen and water vapor dynamics in modified-atmosphere packages." Journal of Food Science, Volume 61, No. 5, 1996.
- [17] Susana C. Fonseca, Fernanda A.R. Oliveira, Isabel B.M. Lino, Jeffrey K. Brecht, Khe V. Chau. "Modelling O₂ and CO exchange for development of perforation-mediated modified atmosphere packaging." Journal of Food Engineering 43 (2000) 9-15.
- [18] Jaime Gonzalez, Ana Ferrer, Rosa Oria, Maria L. Salvador. "Determination of O₂ and CO₂ transmission rates through microperforated films for modified atmosphere packaging of fresh fruits and vegetables." Journal of Food Engineering 86 (2008) 194-201.

- [19] Bruno Flaconnèche, Joseph Martin, M-Helene Klopffer. "Permeability, diffusion and solubility of gases in polyethylene, polyamide 11 and poly(vinylidene fluoride)." *Oil & Gas Science and Technology. IFP*, Vol. 56 (2001) No. 3, pp. 261-278.
- [20] [20] Petri Johansson, Hannu Teisala, Kimmo Lahtinen, Jurkka Kuusipalo. "Protecting an atomic layer deposited aluminum oxide barrier coating on a flexible polymer substrate." *Thin Solid Films* 621 (2017) 151-155.